

Reliability Based Optimal Design of Truss Structures using Binary Particle Swarm Optimization with Time-Varying Parameters

C. K. Dimou, A. E. Charalampakis

Proc. 2nd International Conference on Soft Computing Technology in Civil, Structural and Environmental Engineering (CSC2011), Chania, Greece; 2011.

Abstract

The Binary Particle Swarm Optimization (BPSO) algorithm has been implemented with success in the Reliability Based Optimal Design (RBOD) of truss structures. In this study, a BPSO implementing time-varying schemes for the inertia factor and maximum velocity is used for the same purpose. Various schemes are examined and the performance is compared against the simple BPSO.

Keywords: Reliability Based Optimal Design, Particle Swarm Optimization, time-varying parameters, truss structures.

1 Introduction

Particle Swarm Optimization (PSO) is a population-based stochastic optimization technique suitable for global optimization with no need for direct evaluation of gradients. The method mimics the social behavior of flocks (swarms) of birds and insects [1] and satisfies the five axioms of swarm intelligence, namely; proximity, quality, diverse response, stability and adaptability [2]. The algorithm searches the Design Space (DS) by adjusting the trajectories of individuals, called “particles”, viewed as moving points in the DS. These particles are attracted towards the positions of both their personal best solution and the best solution of the swarm in a stochastic manner [3].

A discrete (binary) version of the algorithm was subsequently introduced [4]. In Binary PSO (BPSO), a chromosome defines a candidate design. Each chromosome contains the necessary information to define a candidate solution of the problem. The main difference of the BPSO as compared to the standard version, is in the use of the information contained in the velocity vector. In PSO the velocity vector is used to calculate the particle’s future position. In BPSO the velocity is used to calculate the probability of the bits of the chromosome to be set either to 0 or 1. Thus, velocity is interpreted as a probability or entrapment threshold. As this

threshold increases, the bit-flip probability decreases and the bit value is locked to either 0 or 1, depending on the sign of the velocity parameter. The BPSO is used mainly in problems of combinatorial nature [5], [6]. Recently, the BPSO was implemented in the area of structural optimization for the Reliability Based Optimal Design (RBOD) of truss structures [7].

The RBOD has attracted the attention of many researchers [8]. In RBOD, part of the constraints and/or the objective function is of a probabilistic nature. Reliability analysis provides a rational basis to quantify safety. A structure is considered safe when *it will not fail under foreseeable demands and it is unlikely to fail under extraordinary demands or circumstances* [9]. In reliability analysis, the yes/no (acceptable/non-acceptable) concept of current codes of practice, with regard to the requirements of a design, is substituted by a probability measure for a particular component of the structure to behave in an unacceptable manner (failure). The advantage of RBOD with respect to typical optimization processes, which are based on the requirements of structural codes and regulations (Level 1 methods), is its ability to overcome the problem of optimal designs with reduced reliability. This often occurs in the case of typical optimization. Wen [10], [11] has demonstrated that redundancy factors, related directly to the acceptable risk, are required to obtain designs of the same level of safety and economy.

Due to its high computational cost, RBOD has only become practical with the advancement of computing hardware [12], [13], [14]. Dimou and Koumousis [15] implement a competitive GA algorithm for the RBOD of truss structures. Youn and Choi [16] address the problem of maximizing the safety of a vehicle in side impacts, while the weight of the safety cell is kept below a certain threshold value. Foley et al. [17], [18] present a state-of-the-art overview of performance-based methodologies in the design of steel moment resisting frames subject to seismic loading while incorporating risk in structural design.

In this work, the RBOD of two statically determinate planar trusses is examined, namely of a 25-bar truss and a 30-bar arch. A modified BPSO is employed for the optimization process. The Design Variables (DVs) are the cross-sectional areas A_i of the groups, which control the size of the truss, and the heights h_j and lengths l_k which control its shape. The problems under examination are modeled as serial systems of partially correlated groups of elements. The Random Variables (RVs) are the load, the yield-critical stress and the cross sections of the elements. The modifications introduced in the BPSO algorithm are inspired by the work of Fourie and Groenwold [19]. These modifications are mainly concerned with the introduction of time-varying schemes for the inertia parameter and the maximum velocity. The results of the proposed schemes are compared with the results of the standard BPSO.

2 Modified Binary PSO

In BPSO, the value of the i^{th} bit is given as [4]:

$$\begin{aligned} x_{k+1}^i &= 1 & r_{k+1}^i &\leq \text{sig}(v_k^i) \\ x_{k+1}^i &= 0 & r_{k+1}^i &> \text{sig}(v_k^i) \end{aligned} \quad \text{where} \quad \text{sig}(v_k^i) = \frac{1}{1 + \exp(-v_k^i)} \quad (1)$$

where the sigmoid function $\text{sig}(v_k^i)$ varies in the range of $[0,1]$ and r_{k+1}^i is a random value uniformly distributed in the range $[0,1]$. The velocity vector is used to derive the probability of the i^{th} bit of the chromosome to be equal to 1. An extended analysis on the behavior of BPSO and its derivations can be found in Clerc [20]. The velocity vector is given as:

$$\mathbf{v}_{k+1}^d = w_k \mathbf{v}_k^d + c_1 \mathbf{r}_1 \circ (\mathbf{p}_k^d - \mathbf{x}_k^d) + c_2 \mathbf{r}_2 \circ (\mathbf{p}_g - \mathbf{x}_k^d) \quad (2)$$

where, w_k is the inertia factor at time instant k ; c_1, c_2 are the cognitive and social parameters of the algorithm, respectively; \mathbf{p}_k^d is the best ever position vector of individual d at time instant k ; \mathbf{p}_g is the best ever position vector amongst all individuals at time instant k ; $\mathbf{r}_1, \mathbf{r}_2$ are vectors of random variables with uniform distribution in the interval $[0,1]$ and the (\circ) operator indicates element-by-element multiplication. The components of the velocity vector are bounded by a maximum velocity v_{\max} . The v_{\max} acts as a maximum entrapment probability, forcing the bit value to either 0 or 1. Every velocity component of \mathbf{v}_k^d is examined against the maximum velocity and the following correction is implemented if needed:

$$\text{if } |v_{k+1,i}^d| > v_{\max} \Rightarrow v_{k+1,i}^d = \text{sign}(v_{k+1,i}^d) \cdot v_{\max} \quad \forall i \in \{1, \dots, N_{DV}\} \quad (3)$$

where N_{DV} is the number of DVs of the problem and $\text{sign}(_)$ is the signum function.

To improve the performance of the BPSO, a series of modifications are implemented. These are proposed by Fourie and Groenwold [19]. The resulting optimization scheme is designated as Enhanced BPSO (EBPSO) and is implemented as follows:

- If the best solution found in the whole swarm is not improved over a period of h consecutive steps, then it is assumed that the current values for the inertia factor and maximum velocity are not suitable. For this reason, both of them are modified as follows:

$$\text{If } OF(\mathbf{p}_g)|_k = OF(\mathbf{p}_g)|_{k-h} \Rightarrow w_{k+1} = f(a w_k), \mathbf{v}_{k+1}^{\max} = g(\beta \mathbf{v}_k^{\max}) \quad (4)$$

where $f(_)$ and $g(_)$ are arbitrary functions.

- The craziness operator assigns a random velocity vector to an individual resulting in its moving away from the swarm and thus exploring other areas. In BPSO this operator resembles the massive mutation operator found in some versions of the Genetic Algorithms (GAs). The operator is activated with a probability P_{cr} as follows:

$$\text{If } r < P_{cr} \Rightarrow \text{randomly assign } \mathbf{v}_{k+1} \text{ with } \mathbf{0} < \mathbf{v}_{k+1} \leq \mathbf{v}_{k+1}^{\max} \quad \forall \text{ particle } d \quad (5)$$

where r is a random variable with uniform distribution in the interval $[0,1]$.

- The algorithm employs both an elite particle and an elite velocity. The individual with the worst performance is moved to the best ever position of the swarm:

$$\mathbf{x}^{pe} = \mathbf{p}_g \quad (6)$$

In addition, if the velocity vector \mathbf{v}_k^d resulted in an improvement of \mathbf{p}_g , then:

$$\mathbf{x}_{k+1}^d = \mathbf{p}_g + c_3 \mathbf{r}_3 \circ \mathbf{v}^{pe} \quad (7)$$

where, $\mathbf{v}^{pe} = \mathbf{v}_k^d$, c_3 is a parameter of the algorithm and \mathbf{r}_3 is a vector of random variables with uniform distribution in the interval $[0,1]$.

The original v_{\max} is not controlled by parameter γ as in [19], but its range is selected following other recommendations found in literature [7]. This is due to the fact that velocity in BPSO is interpreted as a probability and not as a vector that determines the future position of a particle, as in the classical PSO.

3 Reliability Based Optimal Design

The BPSO, as well as other Evolutionary Algorithms like GAs, are particularly suitable for computationally intensive and mathematically hard problems. The main reason is that they only require payoff information. The RBOD is a computational intensive and mathematically hard problem even in its simplest form. As such, it is suitable to reveal the strengths and weaknesses of BPSO and its modifications.

The objective of the problem is to minimize the sum of the construction cost and the cost of potential structural failure [10], [11]. The DVs are the cross-sectional areas A_i of the member groups (taken from a list of available tubular cross sections), as well as the heights h_j and lengths l_k , which control the size and shape of the truss. The constraints consider the failure probabilities of both the elements and the structure. The optimization problem is formulated as follows:

$$\min \quad F(A_i, h_j, l_k) = \underbrace{\sum_{m=1}^{N_t} V_m(A_i, h_j, l_k) \cdot C_{mat}}_{\text{Construction Cost}} + \underbrace{P_{f,s} \cdot C_{fail}}_{\text{Potential Failure Cost}} \quad (8)$$

$$g_n(A_i, h_j, l_k) = \frac{P_{f,n}}{P_{n,\lim}} - 1.0 \leq 0, \quad g_s(A_i, h_j, l_k) = \frac{P_{f,s}}{P_{s,\lim}} - 1.0 \leq 0 \quad (9)$$

where N_t is the number of truss elements, V_m is the volume of the m^{th} element, C_{mat} and C_{fail} are the structural cost per unit volume and the cost of potential structural failure, respectively, $P_{f,n}$ and $P_{n,\lim}$ are the failure probabilities of the n^{th}

element and its maximum failure probability, respectively, and $P_{f,s}$ and $P_{s,lim}$ are the failure probability and its limit value for the entire structure. Note that no construction constraints are taken into account.

The failure probability for an element is defined as the probability of the ratio of resistance over action obtaining values below unity ($P_{f,n}=\Pr(R_n/S_n\leq 1)$). For the problems examined herein, every member force S_n is given as the load acting on the structure multiplied by an appropriate coefficient for each element ($S_n=f_n(h_j,l_k)\cdot P$). For statically determinate structures, the function $f_n(h_j,l_k)$ depends only on the geometry of the design and the load pattern. The expressions listed in EC3 are employed for the tensile and compressive-buckling resistance. The tensile resistance is given as the cross sectional area multiplied by the tensile yield stress ($R_n=\sigma_y\cdot A_n$). The compressive resistance is given as the cross-sectional area multiplied by the reduced critical stress in compression. The latter is given as the compressive yield stress multiplied by a reduction factor χ accounting for buckling, based on the provisions of EC3 ($R_n=\chi_n\cdot\sigma_y\cdot A_n$).

The RVs of the problem are the load P , the yield stress of the material σ_y , the cross sectional areas A_j of all groups of bars and the reduction factors χ accounting for buckling for all groups of bars. All RVs are considered as log-normally distributed; thus, the problem of calculating the failure probability of an element has an analytical solution [15]. The average and coefficient of variation (C.O.V.) of the RVs are summarized in Table 1. The truss elements form four groups, namely the lower and upper chords, the vertical struts and the diagonal members. In every group, the elements are considered as fully correlated; thus, since every group is modeled as a serial system of elements, the failure probability of the group is derived from the maximum of the failure probabilities of the members of the group. The structural failure probability is obtained as the average of the Ditlevsen bounds of the corresponding series of correlated groups.

Two examples are examined which cover the structural behavior of a wide range of statically determinate truss structures, namely a simply supported 25-bar truss (Fig. 1) and a 30-bar 3 hinge arch (Fig. 2) [7]. The data regarding the DVs of the problem is presented in Table 2.

For the 25-bar truss, the total span length is $L=10\text{m}$. The number of DVs for this problem is equal to 13. Four DVs control the size of the truss by selecting the cross-section A_i of each group. Seven DVs are used to determine the h_j of the truss and two DVs are used for the span lengths l_k that control the shape of the truss. For the DVs controlling the A_i and h_j , 4 bits are used to describe each DV whereas for the lengths 3 bits are used. The number of bits needed to fully describe a design is equal to $(4+7)\cdot 4+2\cdot 3=50$; thus, the multiplicity of the DS enumerates 2^{50} designs. A candidate design for the 25-bar truss is described as follows:

0011 0101 0010 1111 0000 1111 0001 0100 0010 1110 0000 000 110												
↓												
Cross Sections				Heights h_j				Lengths l_k				
0011	0101	0010	1111	0000	1111	0001	0100	0010	1110	0000	000	110
↓	↓	↓	↓	↓	↓	↓	↓	↓	↓	↓	↓	↓
L Chord Φ42.7x3.2	U Chord Φ60.1x3.2	Strut Φ33.7x3.2	Diagonal Φ152.4x4.0	0.25m	$h_2=h_1+0.50\text{m}$	$h_3=h_2+0.025\text{m}$	$h_4=h_3+0.10\text{m}$	$h_5=h_4+0.050\text{m}$	$h_6=h_5+0.275\text{m}$	$h_7=h_6$	2.00m	3.50m

For the 30-bar arch, the total span length is $L=13\text{m}$ and the load participation factors $\{a_i\}$ depend on the shape of the structure. The number of DVs for the 30-bar arch is equal to eleven (four control the size of the truss and seven control its shape). For the DVs controlling the A_i and h_j , 4 bits are used to fully describe each DV whereas for the l_k 5 bits are used. The number of bits needed to fully describe a design is equal to $(4+4)\cdot 4+3\cdot 5=51$; thus the multiplicity of the DS enumerates 2^{51} designs. A candidate design for the 30-bar arch is described as follows:

0110|0001|0111|0000|0000|1111|0001|0011|00011|10000|01011

⇓

0110 ↓ L Chord Φ76.1x3.2	0001 ↓ U Chord Φ26.7x2.9	0111 ↓ Strut Φ82.5x3.2	0000 ↓ Diagonal Φ21.3x2.8	0000 ↓ $h_1=1.000\text{m}$	1111 ↓ $h_2=h_1+0.775\text{m}$	0001 ↓ $h_3=h_2-0.150\text{m}$	0011 ↓ $h_4=h_3-0.300\text{m}$	00011 ↓ 3.15m	10000 ↓ 3.30m	01011 ↓ 2.55m
-----------------------------------	-----------------------------------	---------------------------------	------------------------------------	----------------------------------	--------------------------------------	--------------------------------------	--------------------------------------	---------------------	---------------------	---------------------

25-bar truss			30-bar arch		
Random Variable	E [_]	C.O.V	Random Variable	E [_]	C.O.V
Load (kN)	30.0	12.5%	Load (kN)	30.0	25.0%
Yield Stress (MPa)	275.0	7.0%	Yield Stress (MPa)	275.0	7.0%
Cross section (cm ²)	Variable	10.0%	Cross section (cm ²)	Variable	4.0%
buckling factor χ	Calculated	10.0%	buckling factor χ	Calculated	5.0%

Table 1: RVs for the problems examined

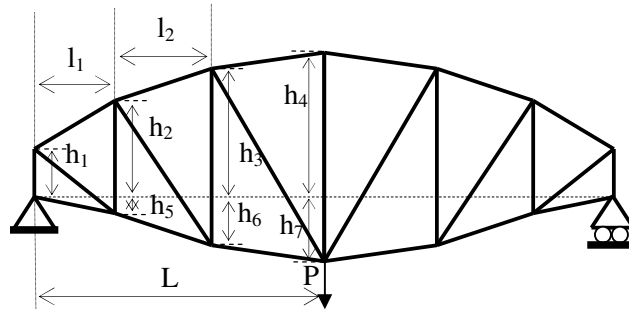


Fig. 1. 25-bar Truss (Load and DVs)

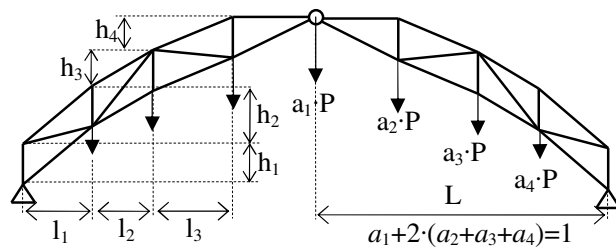


Fig. 2. 30-bar Arch (Load and DVs)

Coding and decoding the binary expressions of all particles is performed at every time step to evaluate the performance of every candidate design, as determined by the optimization problem of eqs. (8) and (9).

CS Name	d	t	CS Name	d	t	CS Name	d	t	CS Name	d	t
Φ21.3x2.8	21.3	2.8	Φ48.4x3.2	48.4	3.2	Φ88.9x3.2	88.9	3.2	Φ127.0x4.0	127.0	4.0
Φ26.7x2.9	26.7	2.9	Φ60.1x3.2	60.1	3.2	Φ101.6x3.6	101.6	3.6	Φ133.0x4.0	133.0	4.0
Φ33.7x3.2	33.7	3.2	Φ76.1x3.2	76.1	3.2	Φ108.0x3.6	108.0	3.6	Φ139.7x4.0	139.7	4.0
Φ42.7x3.2	42.7	3.2	Φ82.5x3.2	82.5	3.2	Φ114.3x3.6	114.3	3.6	Φ152.4x4.0	152.4	4.0
25-bar truss						30-bar arch					
h_1	0.25m to 0.50m Step=0.05m					h_1	From 1.00m to 1.40m Step=0.025m				
	0.50m to 1.50m Step=0.10m						From 1.40m to 2.15m Step=0.050m				
h_2	0.00m to 0.30 Step=0.025m add to h_1					h_2	0.00m to 0.775 Step=0.025m, add to h_1				
	0.30m to 0.50 Step=0.050m add to h_1										
h_3	Values as in h_2 , add to h_2					h_3	-0.175m to 0.60 Step=0.025m, add to h_1				
h_4	Values as in h_2 , add to h_3					h_4	-0.375m to 0.40 Step=0.025m, add to h_1				
h_5	0.00m to 0.30 Step=0.025m					L_1	3.00m to 4.55m Step=0.05m				
h_6	Values as in h_5 , add to h_5					L_2	2.50m to 4.05m Step=0.05m				
h_7	Values as in h_5 , add to h_6					L_3	2.00m to 3.55m Step=0.05m				
L_1, L_2	From 2.00m to 3.75m Step=0.25m										

Table 2. Cross-Sections (CS), heights (h_j) and lengths (l_k)

The ratio of costs is set to $C_{fail}/C_{mat}=200000$ and $P_{n,lim}=10^{-6}$ and $P_{str,lim}=5 \cdot 10^{-6}$. These values correspond to reliability indexes of $\beta_{n,lim}=4.753$ and $\beta_{str,lim}=4.417$ respectively. The $\beta_{str,lim}$ is taken equal to the proposed reliability index in the draft of the Probabilistic Model Code [21] for structures “with small relative cost of safety measure and moderate consequences of failure”. The selection of more stringent limits for the elements is dictated by the type of structure examined. A statically determinate structure has no mechanism to redistribute the acting stresses after failure of any of its elements and its probability of failure is greater than or at least equal to the probability of failure of its most likely to fail element [7].

4 Time-varying schemes for parameters α & β

With respect to the arbitrary functions of eq. (4), the following schemes are examined:

$$\text{If } OF(\mathbf{p}_g)|_k = OF(\mathbf{p}_g)|_{k-h} \text{ then modify } w_{k+1} \text{ and } \mathbf{v}_{k+1} \quad (10)$$

The modifications are performed as follows:

- In the case of the simple ascending or descending scheme (EBPSO#1) as:

$$w_{k+1} = a w_k, \mathbf{v}_{k+1}^{\max} = \beta \mathbf{v}_k^{\max} \quad (11)$$

with $a < 1$ and $\beta < 1$, which define either an increasing or decreasing scheme.

- In the case of the two periodical schemes (EBPSO#2, EBPSO#3) as:

$$\begin{aligned}
w_{k+1} = a w_k \quad \mathbf{v}_{k+1}^{\max} = & \begin{cases} \mathbf{v}_{k+1}^{\max} = \frac{1}{\beta} \cdot \mathbf{v}_k^{\max} & \mathbf{v}_{k+1}^{\max} \leq \mathbf{v}^{\max} & \text{for } \mathbf{v}_k^{\max} \nearrow \\ \mathbf{v}_{k+1}^{\max} = \beta^2 \cdot \mathbf{v}_k^{\max}, w_{k+1} = w_0 & \mathbf{v}_k^{\max} \searrow \\ \mathbf{v}_{k+1}^{\max} = \beta \cdot \mathbf{v}_k^{\max} & \mathbf{v}_{k+1}^{\max} \geq \mathbf{v}^{\min} & \text{for } \mathbf{v}_k^{\max} \searrow \\ \mathbf{v}_{k+1}^{\max} = \frac{1}{\beta^2} \cdot \mathbf{v}_k^{\max}, w_{k+1} = w_0 & \mathbf{v}_k^{\max} \nearrow & \text{for } \mathbf{v}_k^{\max} \nearrow \end{cases} \quad (12) \\
w_{k+1} = a w_k \quad \mathbf{v}_{k+1}^{\max} = & \begin{cases} \mathbf{v}_{k+1}^{\max} = \beta \cdot \mathbf{v}_k^{\max} & \mathbf{v}_{k+1}^{\max} \geq \mathbf{v}^{\min} & \text{for } \mathbf{v}_k^{\max} \searrow \\ \mathbf{v}_{k+1}^{\max} = \frac{1}{\beta^2} \cdot \mathbf{v}_k^{\max}, w_{k+1} = w_0 & \mathbf{v}_k^{\max} \nearrow & \text{for } \mathbf{v}_k^{\max} \searrow \\ \mathbf{v}_{k+1}^{\max} = \frac{1}{\beta} \cdot \mathbf{v}_k^{\max} & \mathbf{v}_{k+1}^{\max} \leq \mathbf{v}^{\max} & \text{for } \mathbf{v}_k^{\max} \nearrow \\ \mathbf{v}_{k+1}^{\max} = \beta^2 \cdot \mathbf{v}_k^{\max}, w_{k+1} = w_0 & \mathbf{v}_k^{\max} \searrow & \text{for } \mathbf{v}_k^{\max} \nearrow \end{cases} \quad (13)
\end{aligned}$$

where \mathbf{v}^{\max} and \mathbf{v}^{\min} are the vectors containing the maximum and minimum values of the maximum velocity, w_0 is the initial value of the inertia factor and $\mathbf{v}_k^{\max} \nearrow$ and $\mathbf{v}_k^{\max} \searrow$ imply that the scheme is in its ascending or descending era. Eq. (12) defines a scheme of ascending and descending periods for the maximum velocity, where eq. (13) defines a scheme of descending and ascending periods for this parameter.

- Finally, two schemes following the Saw-tooth GA [22] (EBPSO#4, EBPSO#5) are considered as:

$$\begin{aligned}
w_{k+1} = a w_k \quad \mathbf{v}_{k+1}^{\max} = & \begin{cases} \mathbf{v}_{k+1}^{\max} = \frac{1}{\beta} \cdot \mathbf{v}_k^{\max} & \mathbf{v}_{k+1}^{\max} \leq \mathbf{v}^{\max} & \beta < 1 \\ \mathbf{v}_{k+1}^{\max} = \mathbf{v}^{\min}, w_{k+1} = w_0 & \text{otherwise} \end{cases} \quad (14) \\
w_{k+1} = a w_k \quad \mathbf{v}_{k+1}^{\max} = & \begin{cases} \mathbf{v}_{k+1}^{\max} = \beta \cdot \mathbf{v}_k^{\max} & \mathbf{v}_{k+1}^{\max} > \mathbf{v}^{\min} & \beta < 1 \\ \mathbf{v}_{k+1}^{\max} = \mathbf{v}^{\max}, w_{k+1} = w_0 & \text{otherwise} \end{cases} \quad (15)
\end{aligned}$$

In Fig. 3, the varying schemes for the inertia factor and the maximum velocity described in eqs (12) to (15) are presented.

4 Parametric studies – numerical results

Numerous parametric studies were performed in order to obtain an in-depth knowledge of the algorithm's behaviour. Regarding the swarm size, the following values are considered: $N_s = \{50, 60, 70, 80, 90, 100\}$. In addition, the following combinations of the cognitive and social parameter are considered: $\{[c_1, c_2]\} = \{[1.5, 2.5], [1.75, 2.25], [2.0, 2.0]\}$, in accordance with the recommendations of

[5] and [7]. The \mathbf{v}^{\max} and \mathbf{v}^{\min} vectors are given as $\mathbf{v}^{\min} = [2.3, 2.3, \dots, 2.3]$ and $\mathbf{v}^{\max} = [5.6, 5.6, \dots, 5.6]$, following the recommendations found in [7]. For the parameters α and β the following values are considered $\alpha = \{1.01, 0.99, 0.98\}$, $\beta = \{0.975, 0.950, 0.925\}$. For the remaining parameters, the following values are considered; $P_{cr} = 0.22$, $h = 3$, $w_0 = \{0.8, 0.9, 1.0\}$ and $c_3 = 1.30$.

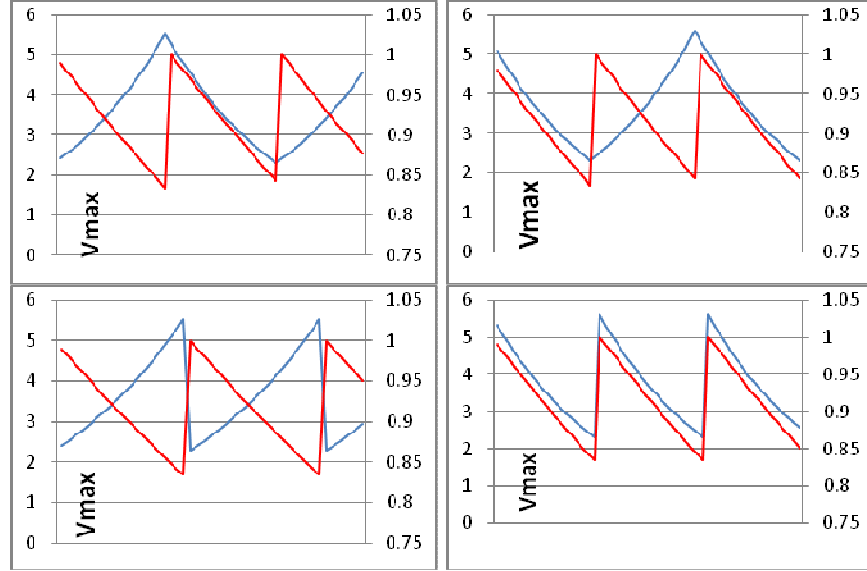


Fig. 3. Varying schemes for the w (red line $\alpha < 1$) and the v_{\max} (blue line $\beta < 1$) – EBPSO#2 to EBPSO#5 from top to bottom and left to right

In total, 2484 combinations of parameters of the BPSO and EBPSO are examined for each truss. For valid statistics, 30 analyses with a different initial random seed are performed for each combination, with a total duration of 200 time steps.

In Fig. 4, the temporal evolution of the best objective over all combinations is presented for both the 25-bar truss and the 30-bar arch. The results for the 25-bar truss are presented on the left side, whereas the corresponding results for the 30-bar arch are given on the right side. For the 25-bar truss, the BPSO and the proposed variants manage to discover the optimum solutions reported in the literature [7], [23]. For the 30-bar arch, the implementation of the proposed variants resulted to new optimal solutions overcoming the ones reported in the literature [7], [23]. The best overall results are observed for the EBPSO#4.

In Fig. 5, the temporal evolution of the best objective is presented when performance is examined against parameter α . Contrary to the results observed for continuous PSO problems [24], for the problems under examination a value above unity gave the best results. This demonstrates the diverse character of the BPSO with respect to its continuous counterpart [19]. Higher values of w increase the importance of the original vector and, in conjunction to higher v_{\max} values, increase considerably the ability of the algorithm to exploit information (as the probability of

bit flip decreases). Note that for $a > 1$ in the corresponding graph at bottom – left of Fig. 3, the red and blue lines are synchronized.

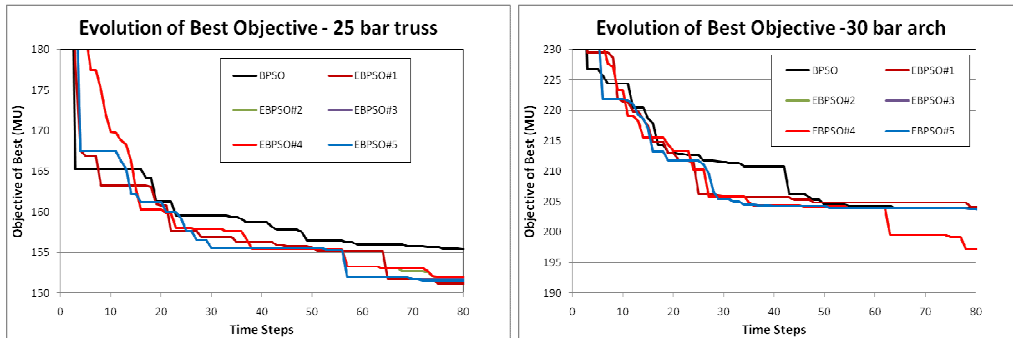


Fig. 4. Evolution of the best objective over all combinations

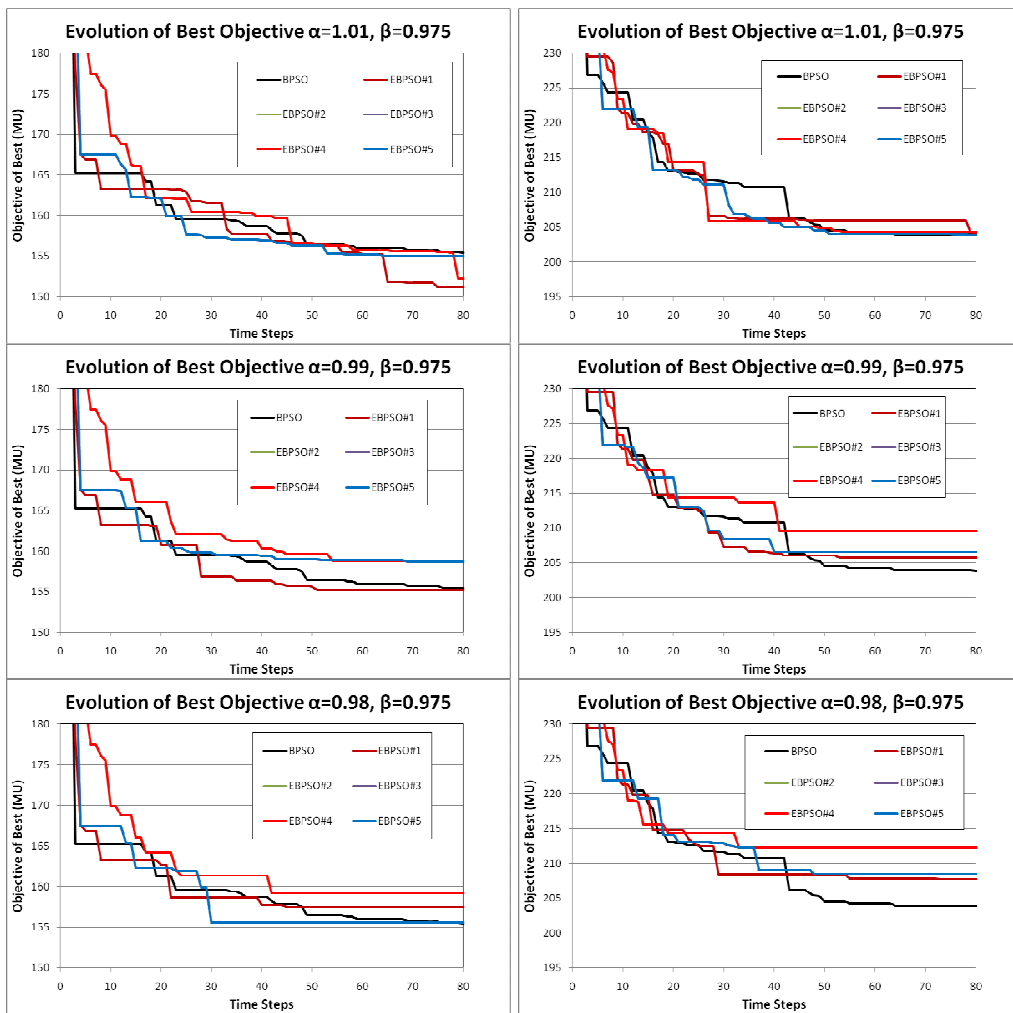


Fig. 5. Evolution of the best objective (performance with respect to the α parameter)

In Fig. 6, the temporal evolution of the best objective is presented when performance is examined against parameter β . In the case of the 25-bar truss, the decrease of β results to a deterioration of performance. This is also the case for the 30-bar arch, although to a lesser degree.

From the results of Fig. 5 and Fig. 6, the best results are observed for $a = 1.01$ and $\beta = 0.975$. Thus, from this point forward, attention is restricted to the results of this specific set of parameter values.

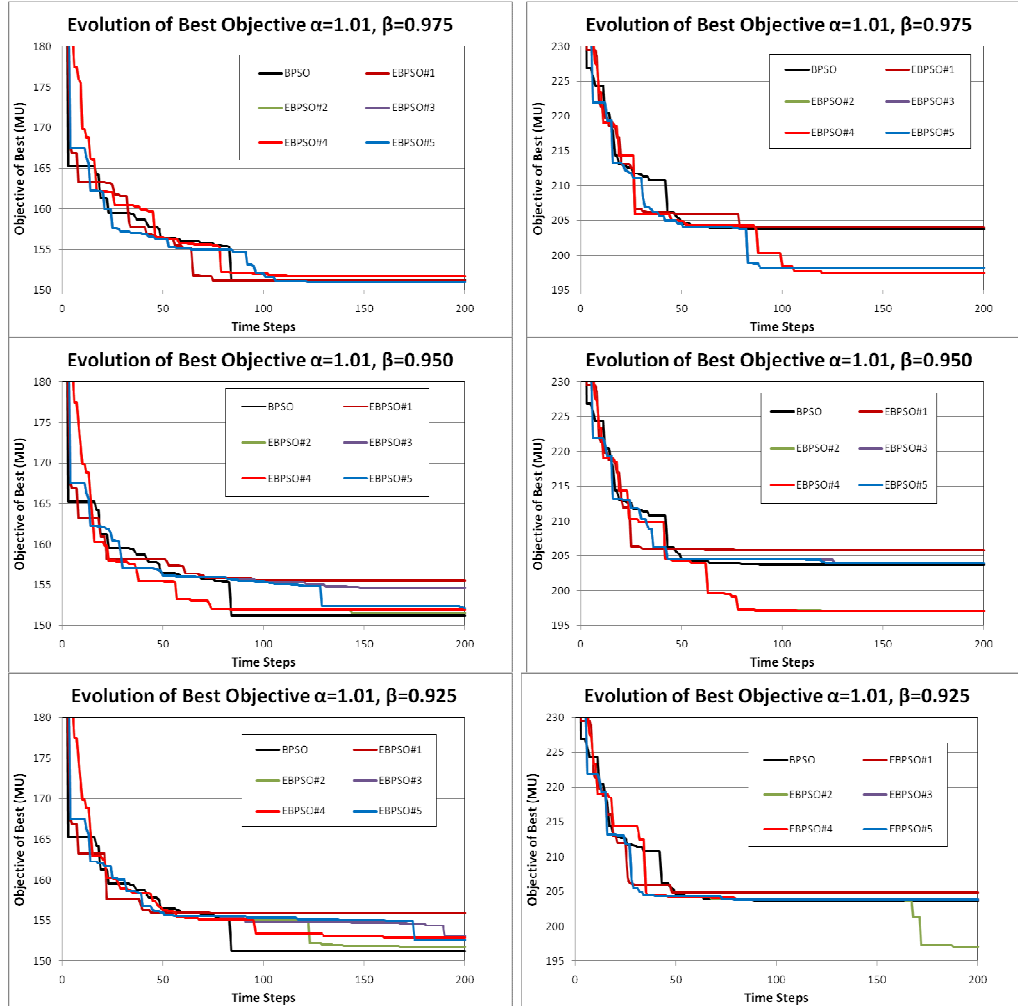


Fig. 6. Evolution of the best objective (performance with respect to the β parameter)

In Fig. 7, the temporal evolution of the mean objective of the optimum particle is presented. At the early stages of the optimization process (up to 40 time steps) the BPSO manages to keep pace with the most efficient EBPSO variants. From that point forward, the ability of the EBPSO for exploitation of the areas where good solutions reside leads to considerable improvements of performance. Moreover, a comparison among the proposed variants shows that EBPSO#4 manages to produce the best results with respect to this metric.

In Fig. 8, the temporal evolution of the “worst” objective of the optimum particle is presented. This metric provides an estimate of the algorithm’s ability to overcome the “faith” of a far-from-optimal original pool of solutions. In BPSO, stagnation is observed as the temporal evolution flat-lines at about 50 time steps. On the other hand, all the examined variants of the EBPSO continue improving until the end of the optimization process. The best performance is observed by EBPSO#4 and EBPSO#1.

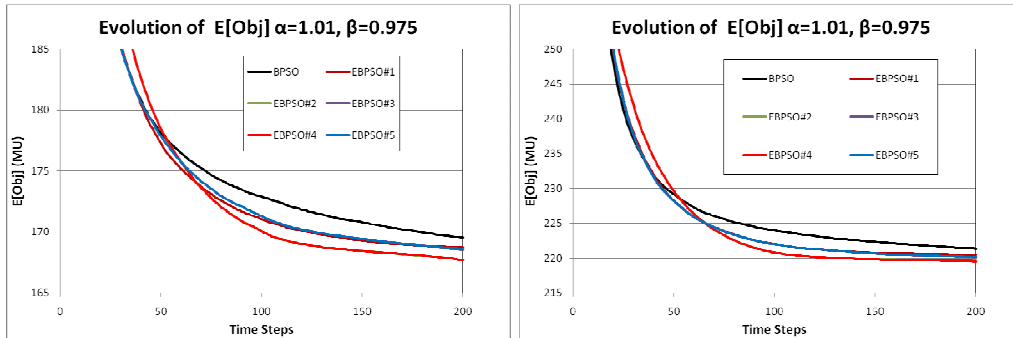


Fig. 7. Evolution of the average objective ($a = 1.01$ & $\beta = 0.975$)

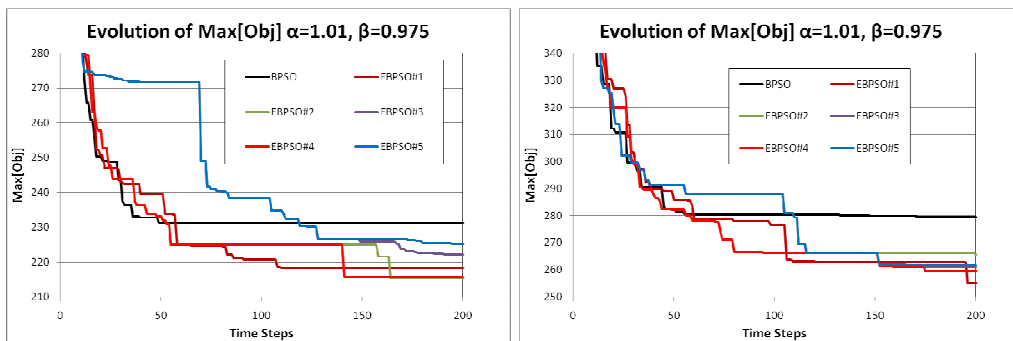


Fig. 8. Evolution of the worst objective ($a = 1.01$ & $\beta = 0.975$)

In Fig. 9, the temporal evolution of the variance of the objective of the optimum particle is presented. This metric provides a better insight with regard to the optimization process. High values indicate increased discrepancy among the results and this is generally considered as beneficial in the early stages of the optimization process. This is not the case at the end of the optimization process when low values of variance indicate that the algorithm is capable of producing consistent results, a clear indication of robustness. These phenomena are observed in the examined graphs. At the early stages of the optimization process the BPSO exhibits lower values of variance when compared to the proposed variants. On the other hand, at the end of the optimization process the exact opposite phenomenon is observed, as the BPSO exhibits the highest variance, a clear indication of entrapment in local optima. The EBPSO#1 and EBPSO#4 produce the best results.

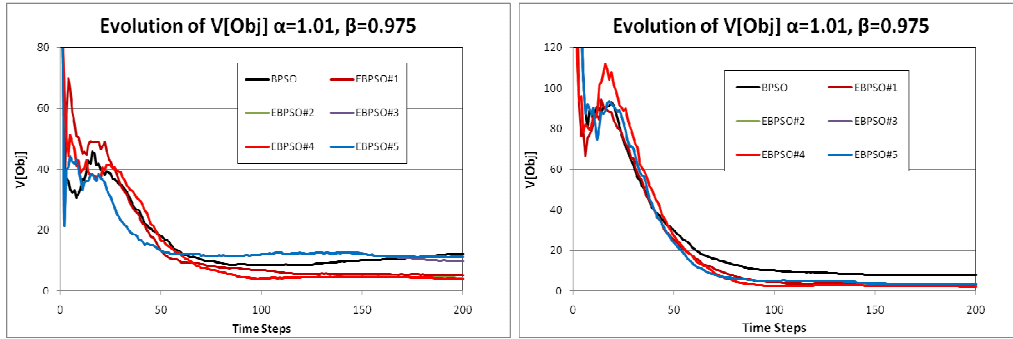


Fig. 9. Evolution of the variance of optimum objective ($a = 1.01$ & $\beta = 0.975$)

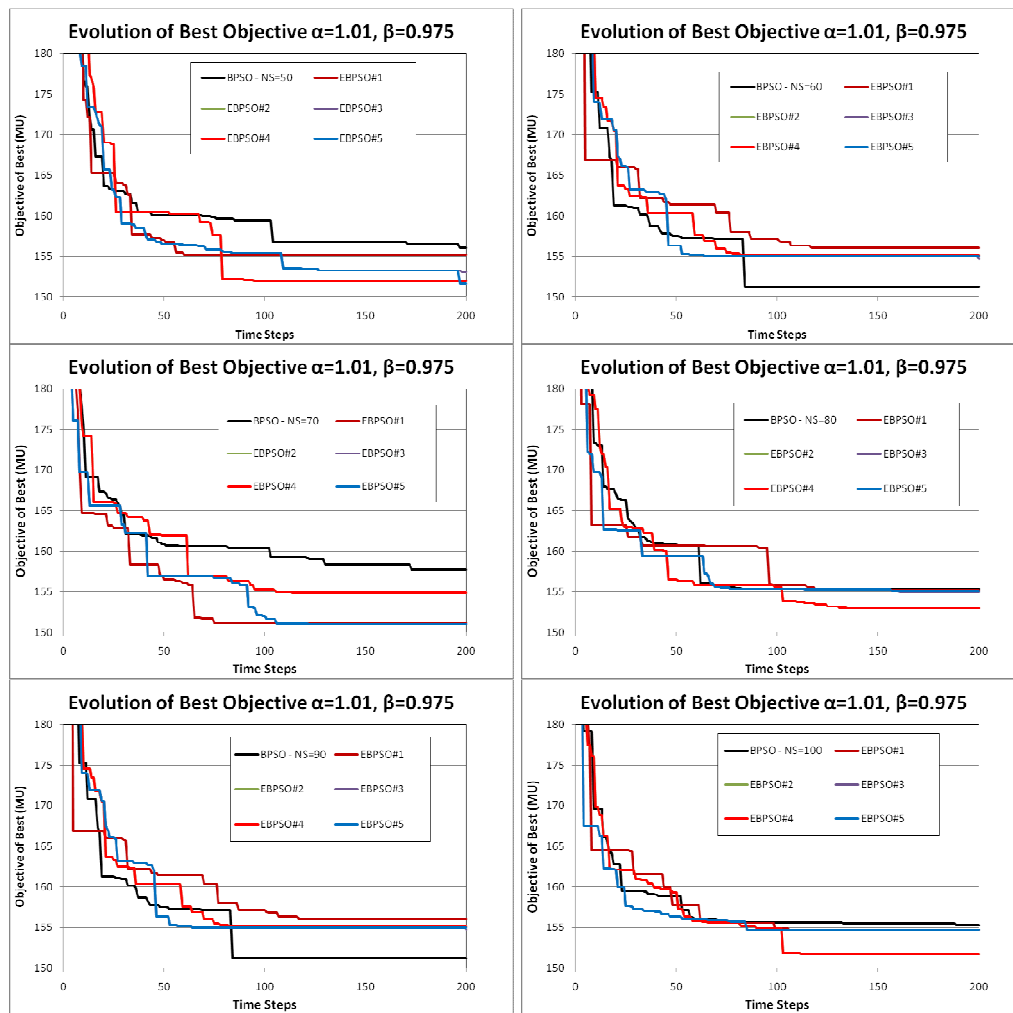


Fig. 10. Evolution of the best objective of the best individual (analysis with respect to $N_s - 25$ bar truss)

In Fig. 10 and Fig. 11, the temporal evolution of the best and average of the objective of the optimum particle is presented for the 25-bar truss, when

performance is examined against the swarm size. In the case of the best objective, the BPSO manages to outperform the proposed variants for $N_S=\{60,90\}$. This is not the case for the average objective, where for all swarm sizes the proposed variants outperform the BPSO. Similar results are also obtained for the 30-bar arch. The best overall results are observed by EBPSO#4.

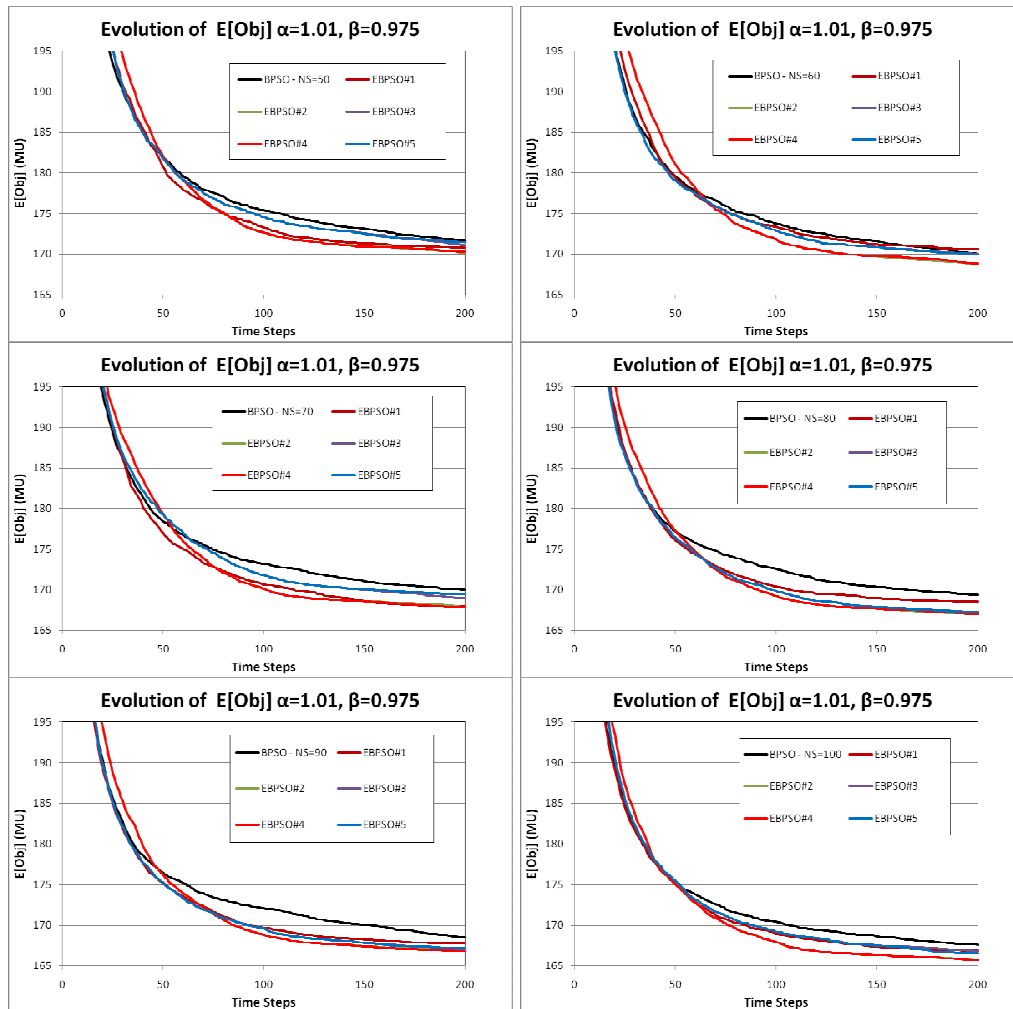


Fig. 11. Evolution of the average objective of the best individual (analysis with respect to N_S – 25 bar truss)

5 Conclusions

In this work, several variants of BPSO incorporating the enhancements proposed by Fourie and Groenwold [19] are implemented in the shape and size RBOD of a 25-bar truss and a 30-bar arch. These structures define two types of structural systems carrying vertical loads which represent two different patterns of structural behavior. The results obtained from these variants are examined against the results of the

BPSO [7].

From the results it becomes evident that the proposed modifications improve considerably the robustness of the algorithm and its exploitation capabilities. For both structures, the best results are obtained with the EBPSO#4 using $a = 1.01$ and $\beta = 0.975$. Thus, the best results are observed for a saw-tooth scheme with gradually increasing maximum velocity and gradually increasing value of the inertia parameter (in synchronization).

References

- [1] J. Kennedy, R.C. Eberhart, "Particle swarm optimization", In "Proceedings of IEEE International Conference on Neural Networks", 1942–1948, 1995.
- [2] M.M. Millonas, "Swarms, Phase Transitions and Collective Intelligence". In "Artificial Life III, Santa Fe Institute, Studies in the Sciences of Complexity, XVII", 417-445, 1994.
- [3] M. Clerc, J. Kennedy, "The Particle Swarm - Explosion, Stability, and Convergence in a Multidimensional Complex Space", IEEE Transactions on Evolutionary Computation, 6(1), 58-73, 2002.
- [4] J. Kennedy, R.C. Eberhart, "A discrete binary version of the particle swarm algorithm", In "Proceedings of the Conference on systems, Man, and cybernetics, Orlando USA", IEEE press, Piscataway, N.J., 4104–4108, 1997.
- [5] N. Franken, A.P. Engelbrecht, "Investigating Binary PSO parameter influence on the Knights Cover Problem" In "The 2005 IEEE Congress on Evolutionary Computation", IEEE Press, Piscataway N.J., 282-289, 2005.
- [6] Y. Gao, Z. Ren, C. Xu., "A Branch and Bound-PSO Hybrid Algorithm for Solving Integer Separable Concave Programming Problems", Applied Mathematical Sciences, 1(11), 517-525, 2007.
- [7] C.K. Dimou, V.K. Koumoussis, "Reliability based optimal design of truss structures using particle swarm optimization", Journal of Computing in Civil Engineering, ASCE, 23, 100-109, 2009.
- [8] Mc Donald M., Mahadevan, S. "Design Optimization with System-Level Reliability Constraints" Journal of Mechanical Design, ASME, 130(2), 021403, DOI:10.1115/1.2813782, 2008.
- [9] D.G. Elms, Achieving Structural Safety: Theoretical Considerations, Structural Safety, 21, 311-333, 1999.
- [10] Y.K. Wen, "Minimum lifecycle cost design under multiple hazards", Reliability Engineering and System Safety, 73 (3), 223-231, 2001.
- [11] Y.K. Wen, "Reliability and Performance based Design", Structural Safety, 23 (4), 407-428, 2001.
- [12] A.H.S. Ang, D. De Leon, "Determination of optimal target reliabilities for design and upgrading of structures", Structural Safety, 19 (1), 91-103, 1997.
- [13] J.O. Royset, A.D. Kiureghian, E. Polak, "Reliability Based Optimal Design of Series Structural Systems", Journal of Engineering Mechanics-ASCE, 127(6), 607-614, 2001.

- [14] C.K.P.V. Thampan, C.S. Krishnamoorthy, "System Reliability-Based Configuration Optimization of Trusses", *Journal of Structural Engineering*, 127 (8), 947-956, 2001.
- [15] C.K. Dimou, V.K. Koumouisis, "Genetic Algorithms in a competitive environment", *Journal of Computing in Civil Engineering*, 17(3), 142-149, 2003.
- [16] B.D. Youn, K.K. Choi, "A new response surface methodology for reliability-based design optimization", *Computers and Structures*, 82(2-3), 241-256, 2004.
- [17] C. Foley, S. Pezeshk, A. Alimoradi, "Probabilistic Performance-Based Optimal Design of Steel Moment-Resisting Frames. I: Formulation", *Journal of Structural Engineering ASCE*, 133 (6), 757-766, 2007.
- [18] C. Foley, S. Pezeshk, A. Alimoradi, "Probabilistic Performance-Based Optimal Design of Steel Moment-Resisting Frames. II: Applications", *Journal of Structural Engineering - ASCE*, 133 (6), 767-776, 2007.
- [19] P.C. Fourie, A.A. Groenwold, "The particle swarm optimization algorithm in size and shape optimization", *Structural and Multidisciplinary Optimization*, 23(4), 259-267, 2002.
- [20] M. Clerc, "Binary Particle Swarm Optimisers: toolbox, derivations, and mathematical insights", http://hal.archives-ouvertes.fr/docs/00/12/28/09/PDF/Binary_PSO.pdf (last accessed Mar. 17, 2011), 2007.
- [21] JCSS, "Probabilistic Model Code, Part 1, Basis of design", 12th Draft, Joint Committee of Structural Safety, http://www.jcss.ethz.ch/publications/publications_pmc.html (last accessed Jan. 2, 2009), 2002.
- [22] V.K. Koumouisis, C.P. Katsaras "A saw-tooth genetic algorithm combining the effects of variable population size and reinitialization to enhance performance", *IEEE Transactions on Evolutionary Computation*, 10, 19-28, 2006.
- [23] C.K. Dimou, V.K. Koumouisis, "Investigation of the Robustness of PSO Algorithms in Reliability Based Optimal Design Problems", In "COMP DYN 2009 - ECCOMAS Thematic Conference", CD434, 2009.
- [24] A.E. Charalampakis, C.K. Dimou, "Identification of Bouc-Wen hysteretic systems using particle swarm optimization", *Computers and Structures*, 88, 1197-1205, 2010.